The Journal of Experimental Biology 216, 4557-4566

doi:10.1242/jeb.092791

RESEARCH ARTICLE

Drastic reorganization of the bioconvection pattern of *Chlamydomonas*: quantitative analysis of the pattern transition response

Azusa Kage, Chiharu Hosoya, Shoji A. Baba and Yoshihiro Mogami*

Graduate School of Humanities and Sciences, Ochanomizu University, Otsuka 2-1-1, Bunkyo-ku, Tokyo 112-8610, Japan

*Author for correspondence (mogami.yoshihiro@ocha.ac.jp)

SUMMARY

Motile aquatic microorganisms are known to self-organize into bioconvection patterns. The swimming activity of a population of microorganisms leads to the emergence of macroscopic patterns of density under the influence of gravity. Although long-term development of the bioconvection pattern is important in order to elucidate the possible integration of physiological functions of individuals through bioconvection pattern formation, little quantitative investigation has been carried out. In the present paper, we present the first quantitative description of long-term behavior of bioconvection of *Chlamydomonas reinhardtii*, particularly focusing on the 'pattern transition response'. The pattern transition response is a sudden breakdown of the steady bioconvection pattern followed by re-formation of the pattern with a decreased wavelength. We found three phases in the pattern formation of the bioconvection of *C. reinhardtii*: onset, steady-state 1 (before the transition) and steady-state 2 (after the transition). In onset, the wavelength of the bioconvection pattern increases with increasing depth, but not in steady-states 1 or 2. By means of the newly developed two-axis view method, we revealed that the population of *C. reinhardtii* moves toward the bottom of the experimental chamber just before the pattern transition. This indicates that the pattern transition response could be caused by enhancement of the gyrotaxis of *C. reinhardtii* as a result of the changes in the balance between the gravitactic and gyrotactic torques. We also found that the bioconvection pattern changes in response to the intensity of red-light illumination, to which *C. reinhardtii* is phototactically insensitive. These facts suggest that the bioconvection pattern has a potential to drastically reorganize its convection structure in response to the physiological processes under the influence of environmental cues.

Supplementary material available online at http://jeb.biologists.org/lookup/suppl/doi:10.1242/jeb.092791/-/DC1

Key words: bioconvection, phase transition, gravitaxis, gyrotaxis.

Received 20 June 2013; Accepted 29 August 2013

INTRODUCTION

Bioconvection is a phenomenon of macroscopic pattern formation that occurs as a result of the collective motion of swimming microorganisms. In a homogeneous suspension, swimming activity of the microorganisms, which is biased by gravitational force, causes the anisotropic, top-heavy vertical stratification of the organisms. The accumulation of the organisms is then fragmented, forming downward plumes of the organisms. This fragmentation leads to patch-like horizontal variation in population density. After this vigorous 'onset' process, suspension enters a sort of 'steady-state' in which the horizontal density variation leads to the formation of macroscopic patterns consisting of polygons or dots regularly arrayed in appearance when viewed from above. The steady-state pattern remains for hours or even days (Wager, 1911), as long as the microorganisms are motile.

Research on bioconvection has so far focused mainly on the 'onset' process of pattern formation. This is partly because this process appears so similar to that of thermal convection that bioconvection could be analyzed in terms of the physical principles. In addition, the 'steady-state' pattern that follows the onset process might be considered to be a kind of 'static' state, in which the upward and downward movement of the population of the organisms is in balance.

Steady-state bioconvection, however, is not in the static state, but has been demonstrated to dynamically respond to external stimuli. Mogami et al. demonstrated that the steady-state bioconvection pattern of the ciliate *Tetrahymena* responded to changes in gravitational acceleration (Mogami et al., 2004): the pattern wavelength decreased with increasing acceleration. They also showed that the gravity-dependent response was different among species and the behavioral mutants of the ciliate. This strongly indicates that the motile properties of individual cells are integrated in the macroscopic response: bioconvection of *Tetrahymena* responded to altered gravity not just as isolated individuals, but as a system. From this, we can speculate that physiological functions of the individual cell other than motility may be integrated through the collective movement of the population under the influence of gravity. That is, it is likely for bioconvection to play a role in the physiology of microorganisms, for example, in terms of cell proliferation and mating, through generation of macroscopic fluid flows.

Quantitative analysis of the macroscopic behavior of microorganisms should help gain insight into the role of bioconvection in biological events. Detailed analyses on the temporal as well as spatial properties of the bioconvection pattern may reveal the ability of the macroscopic pattern to respond to the environmental cues, as shown in the case of the gravity response. However, quantitative analyses (e.g. Bees and Hill, 1997; Williams and Bees, 2011a) have so far tended to focus on the onset and relatively short-term behavior (i.e. <10 min from the onset), and the long-lasting,

steady-state pattern has been analyzed largely in qualitative way (e.g. Wager, 1911; Yamamoto et al., 1992).

Through long-term (>10 min) observation of the steady-state bioconvection of *Chlamydomonas reinhardtii* Dangeard 1888, Akiyama et al. (Akiyama et al., 2005) reported a quite interesting behavior of the steady-state pattern. The behavior, which we call in the present study the 'pattern transition response' instead of the 'pattern alteration response' used in Akiyama et al. (Akiyama et al., 2005), is a sudden decrease in wavelength of the initial steady-state pattern formed in the suspension. The transition response occurs spontaneously, in a manner highly similar to the phase transition found in physical events: a local transition event spreads throughout the entire suspension. Such behavior of the steady-state bioconvection pattern had not so far been reported through experiments and had never been predicted by theoretical studies.

The pattern transition response observed in *C. reinhardtii* suggests that the bioconvection pattern, even though seemingly stable, is not always in a steady-state condition, in which the upward and downward movements of the microorganisms are in balance. It seems rather likely that the pattern is in a state of instability that allows the bioconvection itself to play possible roles in biological function.

In the present study, we made the first quantitative description characterizing the whole process of pattern formation and transition through long-term (>120 min) observations on the steady-state bioconvection of *C. reinhardtii*. Through detailed observation over 2 h, we determined the three phases of bioconvection: onset, steady-state 1 (SS1; before pattern transition) and steady-state 2 (SS2; after the transition). Although the latter two phases are not strictly regarded as 'steady-states', we call these phases 'steady' for simplicity of expression in this paper. We found that, during onset, the pattern wavelength increases with increasing depth, but not in steady states. Second, through simultaneous vertical and horizontal observations (two-axis view), we demonstrated that just before the pattern transition occurs, most of *C. reinhardtii* cells move toward the bottom of the experimental chamber. Finally, we showed that changing the time-averaged intensity of red light can change the pattern wavelength. This is the first quantitative report showing that red light, to which *C. reinhardtii* shows no phototaxis, affects bioconvection patterns.

MATERIALS AND METHODS

Cell culture

Chlamydomonas reinhardtii strain 137c mt– was kept gently aerated for 3 or 4 days in sterile tris-acetate-phosphate (TAP) medium (Harris, 1989) at 25°C under a 12 h:12 h light:dark cycle (photon flux density at light phase, ~120 μmol m^{-1} s^{-1}). To obtain the suspension of a given cell density (1 to 10×10^6 cells ml^{-1}), cells were counted on a Fuchs-Rosenthal hemocytometer, and then diluted with fresh TAP (Akiyama et al., 2005). Experiments were carried out at the middle of the light phase and at ambient temperatures of 20–26°C (in most cases, around 24°C).

Plan-view observation

The cell suspension of a given density was transferred into a flat circular glass chamber with an inner diameter of 94 mm between the top and bottom glass plates (without an air gap), which were separated by plastic spacer of a given height (1 to 8 mm) (for details, see Akiyama et al., 2005). For the description of the time course of the bioconvection pattern formation and its transient response, we defined time 0 as the time when the transfer of the suspension was completed.

Top-view images of the bioconvection patterns were taken at a rate of 0.1 frames s^{-1} (i.e. 1 image per 10 s) using a high-definition camcorder (HDR-HC1, Sony, Tokyo, Japan). The image size was 1920×1440 pixels on a grayscale with 256 shades of gray.

The experimental chamber was illuminated from the bottom with a flat light viewer (MedaLight LP-100, Minato Shokai Co., Yokohama, Japan). Wavelengths of <640 nm were cut out with a sharp cut filter (SC-64, Fujifilm, Tokyo, Japan). Under such an illumination condition, *C. reinhardtii* is known to show no phototactic response (Matsuda et al., 1998). Taken under transmissive illumination, the dark region of the obtained image corresponds to the region where *C. reinhardtii* densely accumulates.

For long-term recordings, we used intermittent lighting (IL) in which the light was on for 3.3 s during 10 s of the recording interval to minimize the non-tactic photoresponse, e.g. photosynthesis. In some experiments, continuous lighting (CL) was used to increase the time-averaged illumination intensity, which may regain the photoresponse. In order to reduce the illumination intensity, neutral density (ND) filters (ND-0.3, Fujifilm) were used in addition to the sharp cut filter. For the comparison of the effects of reduced illumination intensity, one cell suspension prepared from a single culture was divided and transferred into two separate chambers: one was illuminated with the ND filter and the other without the ND filter. Bioconvection patterns of these two chambers were recorded simultaneously under the same illumination source (Light Viewer 7000 PRO, Hakuba Photo Industry Co., Tokyo, Japan) with a photon flux density of 1 μmol m^{-1} s^{-1} (light intensity: 20 lx without an ND filter).

Image analysis

For plan-view observations, pattern wave numbers were calculated using the two-dimensional fast Fourier transform (2D-FFT) method (Bees and Hill, 1997; Mogami et al., 2004). For each individual image of the bioconvection pattern, 2D-FFT was conducted using the custom-made image analysis software Bohboh (Bohbohsoft, Tokyo, Japan), and the Fourier spectrum was obtained. To calculate the representative value of the wave number (spatial frequency) of an image, a Gaussian function was fitted to the Fourier spectrum using the least-square method. The peak value of the Gaussian function was regarded as the dominant wave number of the image, i.e. reciprocal of the wavelength of the pattern. In the following, 'wave number' refers to the dominant wave number, for simplicity.

In order to understand the bulk motion of *C. reinhardtii*, we used the space–time plot method as in Kage et al. (Kage et al., 2011). Following the method introduced by Mogami et al. (Mogami et al., 2004), a narrow rectangular region was cut out from a stack of images and then the regions were pasted together following the time sequence. The space–time plot has the dimensions of time and space, representing the temporal change of the given region.

Two-axis view

To examine the vertical as well as the horizontal movement of the *C. reinhardtii* population, we developed the two-axis view system (Fig. 1), in which we can observe bioconvection from the top and from the side simultaneously. A quartz glass cell of inner dimensions 3×3×40 mm (height × depth × width) was used as an experimental chamber. Two cold cathode fluorescent lamps were used as light sources, which were arranged to pass light through a ~0.5 mm slit with a sharp cut filter (SC-64). Top- and side-view images obtained with CCD cameras (XC-ES50, Sony) were mixed with a multiviewer (MV-40F, FOR-A Company, Tokyo, Japan) and recorded with a portable recorder (D-motion DVR-2100, Asiacorp International,

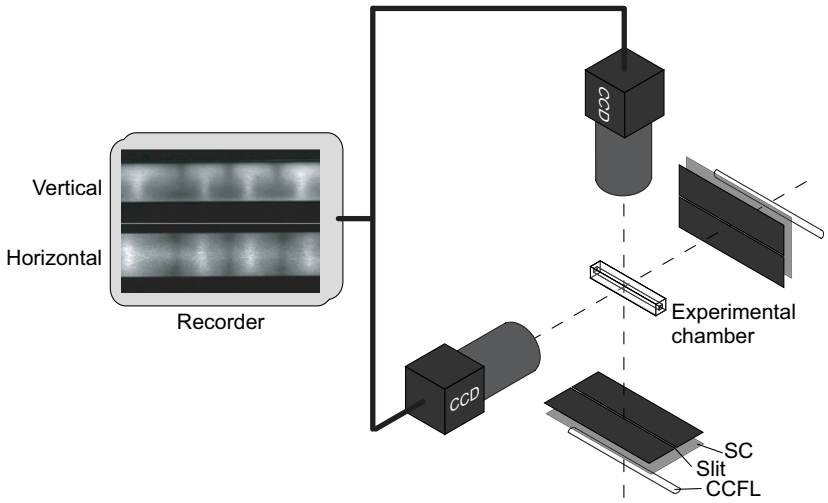

Fig. 1. Experimental setup of the two-axis observation. Specimens in an experimental chamber of 3×3×40 mm were observed simultaneously with two CCD cameras, one from the top (horizontal observation) and one from the side (vertical observation). CCFL: cold cathode fluorescent lamp; SC: sharp cut filter SC-64 (λ>640 nm).

Hong Kong) at a rate of 30 frames s^{-1} and with an image size of 640×320 pixels. In this way we can synchronize the top- and side-view images.

Statistics

In order to assess the effect of suspension depth and cell density on the wave number of the convection pattern, we used the Kruskal–Wallis test, a nonparametric counterpart of the one-way ANOVA. In addition, in order to determine whether the values show an increasing or a decreasing trend, we used the Spearman's rank correlation. The statistical analysis was carried out using R (www.r-project.org).

RESULTS

Pattern formation and the spontaneous pattern transition response

As reported in the previous paper (Akiyama et al., 2005), we found a dynamic behavior of the bioconvection pattern of *C. reinhardtii*. It was revealed in the frame-by-frame analysis of long-term (>30 min) recordings in which the bioconvection pattern suddenly changed its wavelength. We call this transient change the 'pattern transition response'.

Fig. 2 and supplementary material Movie 1 show a typical example of bioconvection pattern formation of *C. reinhardtii*. Sequential images of the plan views of the bioconvection pattern and the corresponding changes in wave number of the pattern image assessed by 2D-FFT are shown in Fig. 2A and 2B, respectively.

The pattern emerged in the homogeneous suspension (Fig. 2A, 0 min) as a local accumulation of the cells in a rectilinear pattern (Fig. 2A, 0.5 and 1 min). This onset pattern gradually changed its shape and developed into a stable pattern, a regular array of dark dots surrounded by bright reticular lines (Fig. 2A, 5, 18 and 21 min). For several (sometimes several tens of) minutes this pattern remained in a steady state, and then a vigorous change occurred. The latter was observed as a local change in the steady-state pattern, in which the dark dots in the stable pattern spontaneously fragmented into smaller dots (Fig. 2A, 22 min, left side). This fragmentation of the pattern unit propagated throughout the suspension (Fig. 2A, 22 and 23 min). From the fragmented, less-organized state (Fig. 2A, 24, 25 and 28 min), another stable pattern was formed (Fig. 2A, 30 and 40 min), which remained stable for more than a couple of hours as long as the cells were motile (Fig. 2A, 60 and 90 min).

The wave number of the plan-view image was small at the onset of the bioconvection pattern and gradually increased to reach a plateau, corresponding to the formation of the stable bioconvection pattern. The wave number suddenly increased further to another plateau through a spike-like transient, corresponding to the transition between steady-state patterns through the propagation of the spontaneous fragmentation of the convection cell.

The transitional event of the bioconvection pattern in the bulk of the *C. reinhardtii* suspension is summarized in the space–time plot (Fig. 2C). The plot, a so-called kymographic or slit camera presentation, shows two regions with a distinct spacing of stripes, representing the pattern transition response in the wavelength of the bioconvection pattern. Between these regions there exists a transitional zone where the stripes appear disordered. The beginning of this transitional zone is slightly delayed in the upper part of the figure, which indicates the propagation of the transitional event (Fig. 2B, 22 to 23 min).

In the present paper we focused our attention on the bioconvection pattern of the three distinct phases: onset and the two steady states, SS1 and SS2, before and after the transition, respectively (Fig. 2B).

Fig. 3 summarizes the measurement of the wave number of the convection pattern at the three different phases. Values were obtained from separate experiments using fixed parameters (suspension depth: 4 mm; cell density: 1×10^7 cells ml^{-1}). Under these conditions, the spontaneous pattern transition response occurred after 10.2±7.5 min (mean ± s.d., N=18) from time 0. The wave numbers measured in SS1 and SS2 showed a larger variation among samples than those measured in the onset phase. No significant correlation was found between the wave numbers of the onset pattern and those of the steady-state patterns (Fig. 3A). However, wave numbers of SS1 and SS2 showed a significant correlation at the 5% significance level (Pearson's product moment correlation, R=0.59, P=0.015, N=16; Fig. 3B). Wave numbers of SS2 were approximately 1.4–1.8 times larger than those of SS1. This tendency was maintained even when we changed the depth and density of cell suspension (see below). In some cases (two out of 18 experiments), the transition occurred so quickly that we could not confirm the SS1 pattern before the transition.

Bees and Hill have reported that both the depth and density of cell suspension have an effect on wavelength of 'initial' and 'final' patterns of bioconvection (Bees and Hill, 1997). We examined the effect of these factors on long-term behavior, including the pattern transition response. The wave number of the onset pattern (Fig. 4A)

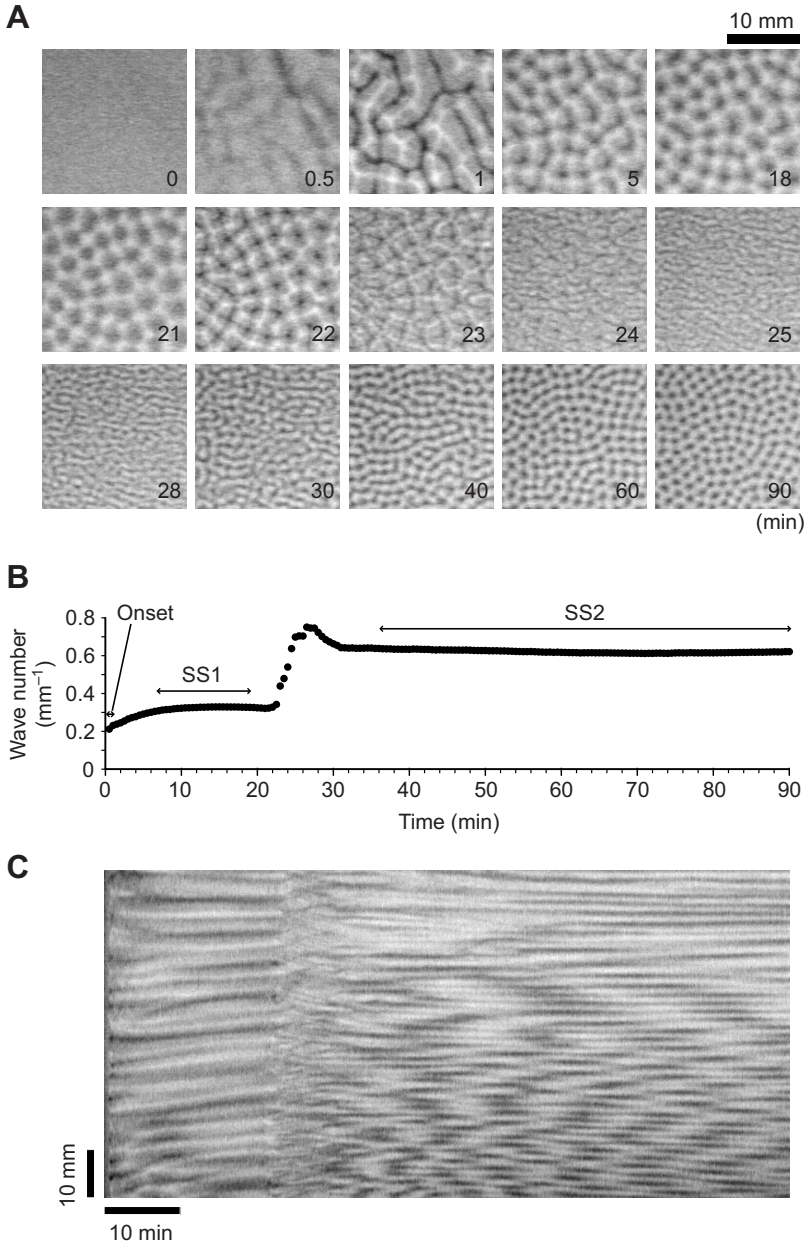

Fig. 2. Long-term development of a typical bioconvection pattern of *Chlamydomonas reinhardtii*. (A) Snapshots of the bioconvection pattern (plan-view). Numbers indicate the time in minutes after the transfer of the cell suspension into the experimental chamber. (B) Long-term change of the pattern wave number obtained from the images shown in A. Dominant wave number (spatial frequency) calculated by the 2D-FFT analysis is plotted against the time after the transfer of the cell suspension. We focused on three distinct phases of pattern formation: onset, steady-state 1 (SS1) and steady-state 2 (SS2). (C) Space–time plot demonstrating the transitional event of the bioconvection pattern of the bulk of the *C. reinhardtii* suspension. Time axis (abscissa) is common to that in B. Suspension depth: 4 mm; cell density: 1.0×10^7 cells ml^{-1}. See supplementary material Movie 1.

showed a clear decreasing trend with increasing suspension depth ($r_S\approx-0.9$, $P<10^{-4}$ for all density conditions), as reported previously (Bees and Hill, 1997). However, the effect of suspension depth was different for the SS1 and SS2 patterns. Kruskal–Wallis *P*-values shown in Fig. 4B indicate that the wave number of the SS1 and SS2 patterns was likely to be insensitive to changes in suspension depth.

Cell density of the suspension had less of an effect than suspension depth on the wave number of both the onset and steady-state patterns. The onset pattern wave number did not show any clear increasing or decreasing trend with increasing density, except for the slight increasing trend at a suspension depth of 2 mm (Kruskal–Wallis, $P=0.0036$; $r_S=0.68$, $P<10^{-4}$). Wave numbers of SS1 and SS2 tended to increase with increasing cell density, although not always with statistical significance [for SS1 and SS2, three and one out of the four different suspension depth conditions were statistically significant (Kruskal–Wallis, $P<0.05$), respectively]. For the data sets that showed significance in the Kruskal–Wallis test, we calculated the Spearman rank correlation coefficient and its *P*-value: the coefficients were around 0.7 and the *P*-values were less than 0.01.

In contrast to the effect on wave number, cell density had a clear effect on the initiation time of pattern transition response. When lowering the density, the transition occurred significantly later (Fig. 5). Suspension depth had little effect on the initiation time of the pattern transition response (Kruskal–Wallis, $P>0.1$ for each cell density condition).

Two-axis view

Because the development of the two-dimensional pattern is the result of the vertical convection of the cell population, analysis of the vertical movement is required to understand the basic mechanism of the pattern transition response. Several trials have been conducted to analyze the vertical convective movement (Harashima et al., 1988; Kitsunezaki et al., 2007). In these experiments, the vertical movement was assessed alone and not in combination with the horizontal development of the bioconvection pattern. In the present

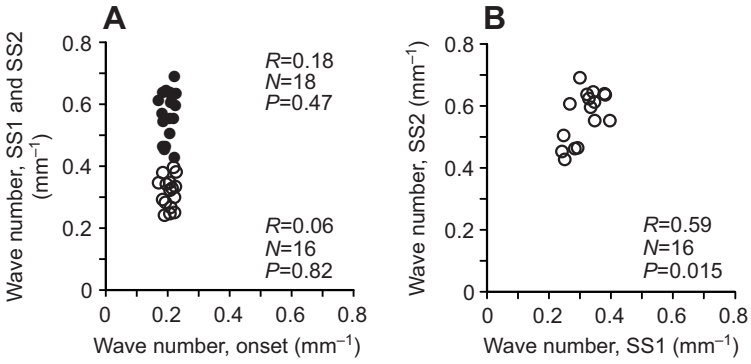

Fig. 3. Pattern wave numbers obtained from the images of the three phases of bioconvection. (A) Pattern wave numbers of SS1 (open circles) and SS2 (filled circles) as a function of the wave number of the onset phase. (B) Pattern wave numbers of SS2 as a function of the wave number of SS1. Pearson's correlation coefficient (*R*) of each plot is shown with *P*-values and sample size (*N*). Suspension depth: 4 mm; cell density: 1.0×10^7 cells ml^{-1}.

study, we introduced an observation method that makes possible the simultaneous recording of the horizontal and vertical movement of the cell population.

In previous experiments we used a quasi-planer vertical chamber for the observation of vertical convective movement (Hosoya et al., 2010; Kage et al., 2011). In a narrow chamber (1 mm width), downward plumes were formed in suspensions of *C. reinhardtii* as well as *Tetrahymena*, which allowed us to observe the vertical movement of the cell populations. In altered gravity during the parabolic flight, the plumes were observed to change their shapes and the position in the chamber in response to the changes in gravitational acceleration (Kage et al., 2011).

Although the horizontally narrow configuration of the chamber is useful for the quantitative observation of the plumes, the pattern transition response hardly occurs in such a narrow chamber. In the present study, we increased the width of the vertical observation chamber to 3 mm, comparable to the spacing of the pattern developed horizontally in a Petri dish (see below), so that the pattern transition events were reproducibly induced and simultaneously recorded in the horizontal as well as vertical directions through the flat glass walls (Fig. 1). An example of the entire recording is shown in supplementary material Movie 2.

In the horizontal observation (Fig. 6A, left column), pattern formation was initiated near the wall of the chamber (Fig. 6A, 2 min). Then the pattern reached a steady state (Fig. 6A, 5 min), although the shape of the pattern was not identical to that of SS1 described above (Fig. 2A). Hereafter, the pattern began to change: the center of the aggregation blob became sharper, and then blobs became fragmented (Fig. 6A, 10–14 min). Later the pattern reached a new steady state where the pattern wavelength decreased compared with the former steady state. This behavior is quite similar to the pattern transition response observed in the conventional flat horizontal chamber. In the present chamber configuration, the transition was initiated 20.6±13.1 min after the

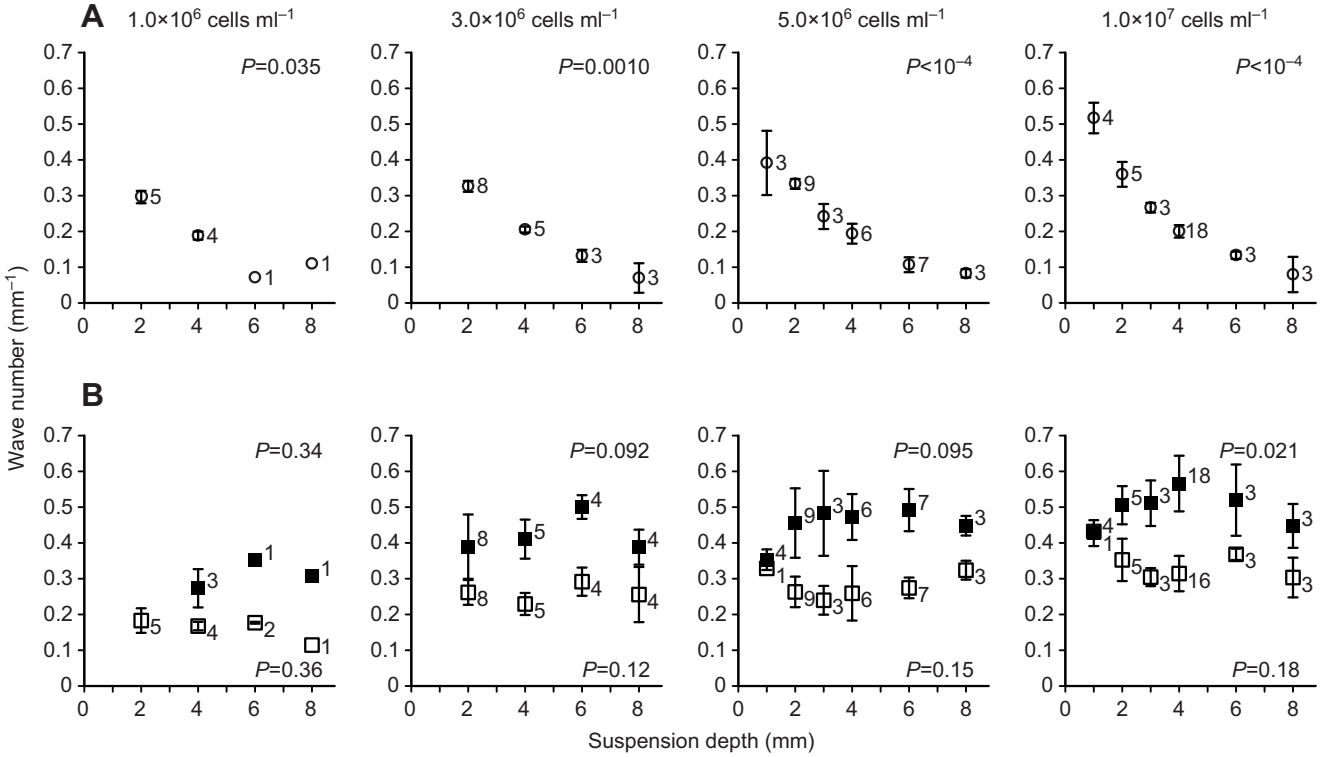

Fig. 4. Effects of suspension depth and cell density on pattern wave number in the three phases of bioconvection. (A) Wave numbers of the onset phase (means ± s.d.) measured in four different densities of cell suspension plotted against suspension depth. (B) Wave numbers of SS1 (open squares) and SS2 (filled squares) measured in four different densities of cell suspension plotted against suspension depth. The significance level of the trends (dependency) obtained by the Kruskal–Wallis test is shown for each plot. The numbers beside the data points represent the number of samples.

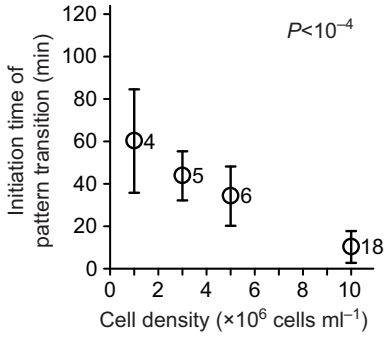

Fig. 5. Effect of cell density on the initiation time of the pattern transition response. Time from the transfer of the suspension to the initiation of the transition (means ± s.d.) is plotted as a function of the cell density of the suspension. The significance level of the trends (dependency) obtained by the Kruskal–Wallis test is shown. Suspension depth: 4 mm. The numbers beside the data points represent the number of samples.

experiment started (mean ± s.d., N=5). In relation to the two-dimensional observation, we call these two states SS1 and SS2, before and after the transition, respectively.

Vertical observation (Fig. 6A, left column) showed that the onset of pattern formation occurs after the accumulation of the cells at the top of the chamber (0–2 min), as reported in previous studies (Hosoya et al., 2010; Kage et al., 2011). It also showed that the 'bottle-shaped' settling blobs are formed in SS1 (Fig. 6A, 5 min), as reported previously (Hosoya et al., 2010; Kage et al., 2011). At the moment the pattern transition response occurred (Fig. 6A, 10–14 min), the 'neck' of the bottle-shaped blobs became constricted, and then a large portion of the *C. reinhardtii* cells migrated downwards, corresponding to the fragmentation of blobs in the horizontal observation. In the SS2 attained after the downward migration, the number of settling blobs increased compared with SS1 (Fig. 6A, 25 min). The mean (±s.d.) spacing between settling blobs was 3.42±0.40 mm for SS1 and 1.79±0.27 mm for SS2 (N=5 for each phase). These values agree well with the wavelengths (the reciprocal of the wave numbers) recorded during the horizontal observation at the same depth and cell density conditions (depth: 3 mm; density: 1×10^7 cells ml^{-1}), which were 3.30±0.27 and 1.98±0.24 mm for SS1 and SS2, respectively (N=3 for each phase).

Space–time plots (Fig. 6B–D) also show that at the beginning of the pattern transition response, the cells moved abruptly downwards. This is clearly demonstrated by the emergence of the bright portion in the space–time plot at the top of the chamber (indicated by an arrow in Fig. 6B), which is due to the dispersal of the cells. In contrast, the plot obtained at the bottom of the chamber shows the dark portion corresponding to the accumulation of the cells (Fig. 6C).

Light-intensity-dependent changes in pattern wavelength

We found a rapid decrease in wave number in the pattern in the SS2 phase when we changed the illumination conditions from IL to CL (Fig. 7A). This change was reversible; the pattern wave number changed depending on the changes in illumination conditions between IL and CL (Fig. 7B). In contrast to the spontaneous pattern transition response, this illumination-type-dependent change in pattern wave number occurred without the accompanying spike-like transient increase in wave number that was usually found at the beginning of the pattern transition response (see Figs 2, 7). It took 5–10 min for the pattern to adapt to the altered illumination and to respond to the next change. The pattern wavelength was observed to change all over the suspension at once, so that we could not observe the propagation of the transition event, which was the second feature of the spontaneous pattern transition response described above. The effect of the illumination conditions was restricted to SS2; the bioconvection pattern in SS1 was not affected by time-averaged light intensity.

In order to assess the effect of the illumination conditions on bioconvection pattern formation, we attenuated the light intensity using ND filters (Fig. 7C). In most cases (eight of nine independent experiments), the wave number of the SS2 pattern was larger when light was attenuated with the ND filter (paired t-test, P=0.00047; Fig. 7C), while the wave numbers of the onset and SS1 patterns and were not clearly affected (paired t-test, onset: P=0.12, SS1: P=0.55). The initiation time of pattern transition response seems to be barely affected by the illumination conditions (P=0.098, paired t-test). In three out of nine experiments, the pattern transition response occurred earlier in the samples with the ND filter, as shown in Fig. 7C. In the remaining six experiments, those without the ND filter showed the pattern transition earlier than their counterparts. The wave number of each phase and the time when the transition occurred are shown in Fig. 7D. Only SS2 showed a significant difference in wave number (paired t-test), and there was no significant difference in transition time. When the ND filter was inserted in the midst of SS2 under CL, the SS2 pattern wave number increased (120±3% compared with before and after insertion; mean ± s.d.; N=4). These findings indicate that changes in wave number are largely due to the changes in the time-averaged intensity of the light; the bioconvection pattern in SS2 reversibly changes its pattern wavelength in response to the total amount of light per unit time.

DISCUSSION

Physical mechanisms of bioconvection

In the present paper we describe quantitatively the pattern transition response of *C. reinhardtii*. 2D-FFT analysis showed that the wave numbers of the steady-state pattern were almost insensitive to the suspension depth and the average cell density of the suspension, while those of the onset pattern were very sensitive to the suspension depth, and decreased with an increase in depth. This sensitivity of wave number to suspension depth and cell density are generally in line with the results of Bees and Hill (Bees and Hill, 1997), who reported that the onset wavelength increases with increasing depth and the 'final' wavelength decreases with increasing density.

The difference in the sensitivity of the pattern wavelength to the suspension depth found between the onset and steady-state patterns could be explained in terms of the physical theories proposed so far. Bioconvection has been explained as being caused by the upward migration of the microorganism, which is purely a result of its physical properties. There have been principally two theoretical models proposed for the formation of the bioconvection pattern, especially at the onset of bioconvection.

The 'density instability model' (Childress et al., 1975; Levandowsky et al., 1975) can be regarded as a general model of bioconvection, irrespective of the species of microorganism. The top accumulation of microorganisms as the result of negative gravitaxis causes instability in the stratification of the fluid density. When the dense, microorganism-containing fluid at the top of the water column starts to settle down, this settling motion induces the onset of the bioconvection, which develops into the regular spatial patterns consisting of downward flow of the accumulated organisms and upward flow of the negatively gravitactically swimming organisms.

The onset of bioconvection has also been explained by another theoretical model, termed the 'gyrotactic instability model'.

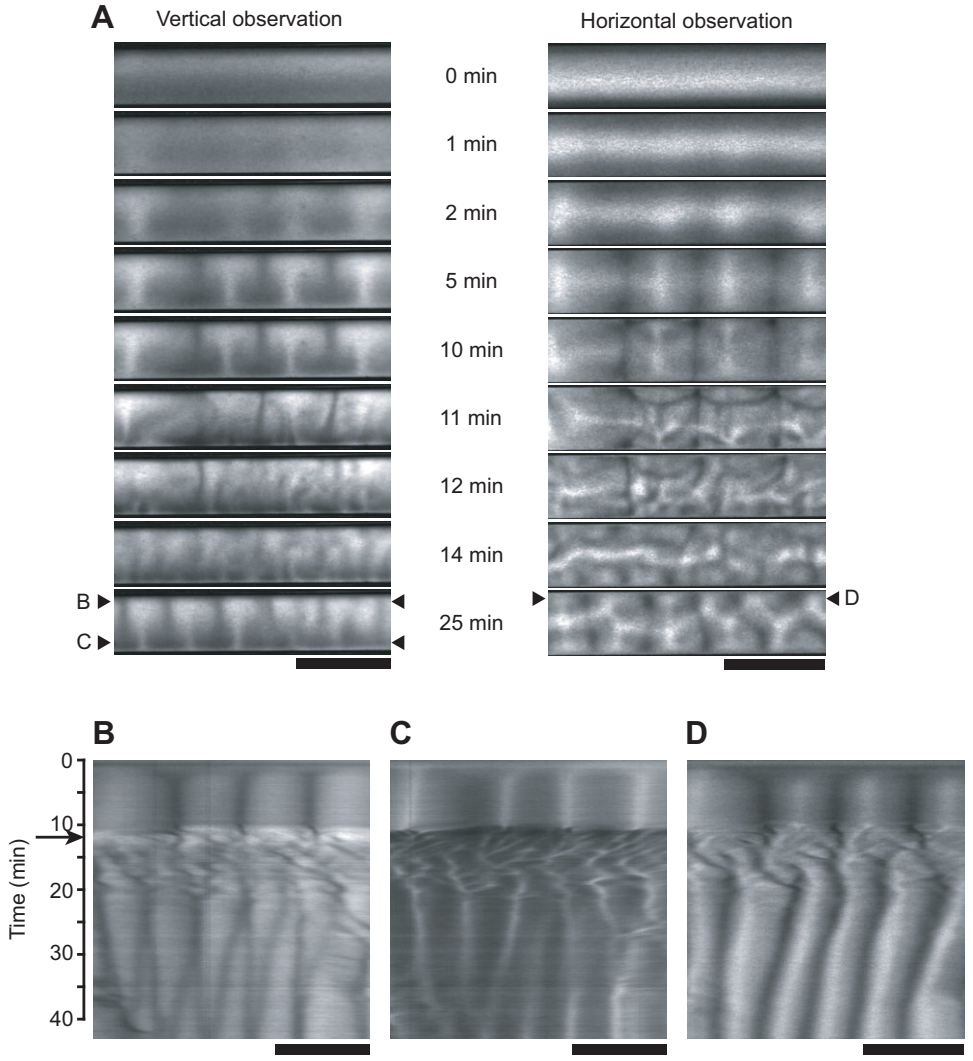

Fig. 6. Two-axis view recording of the pattern transition response. (A) Snapshots of a bioconvection pattern obtained by the two-axis observation showing the images from the vertical observation (side view, left column) and the horizontal observation (top view, right column) with respect to the same time sequence from the start of the experiment (0 min) to steady-state pattern formation (25 min) following the pattern transition response (11–14 min). Faced triangles marked B to D indicate the positions from which space–time plots are made. (B–D) Space–time plots obtained from a portion of the vertical images (B and C from the top and the bottom portion, respectively) and the horizontal image (D) shown in A. The arrow indicates the bright appearance in the top (B) and the dark appearance in the bottom (C) of the chamber. Scale bars, 5 mm. See supplementary material Movie 2.

Gyrotaxis is a biased swimming behavior specific to some gravitactic microalgae such as *Chlamydomonas* (Kessler, 1985b). It causes the algae to reorient based on the torque due to vorticity in the shear flow (gyrotactic torque), in combination with the upward-orienting torque (gravitactic torque) possibly generated by the posterior shift of the center of gravity (Kessler, 1985a; Kessler, 1985b). As a result, gyrotaxis causes *Chlamydomonas* to move towards the downward flow and away from the upward flow. This distinct swimming behavior leads to a local accumulation of the organisms, which would cause the instability to induce large downward flow of the organisms. In this model, bioconvection begins with random flows, and density instability is not always necessary for the initiation of the convection.

Gyrotaxis may cause the pattern transition response

Hopkins and Fauci (Hopkins and Fauci, 2002) conducted numerical simulations of bioconvection, considering the effect of negative gravitaxis, gyrotaxis and chemotaxis. In their simulation work, microorganisms were treated as a discrete point source of mass, the movement of which was affected by the fluid flow governed by the continuous Navier–Stokes equation. The discrete representation of microorganisms, as a result, facilitated the direct evaluation of cell orientation induced by the torques of gravitactic, gyrotactic and chemotactic origin. The simulation, performed with several tens of thousands of particles in the vertical plane, demonstrated the initial overturning of the top accumulation to form downward plumes. Simulations of the 'purely geotactic' particles showed that the wave number, the reciprocal of the plume spacing, decreased with an increase in suspension depth, while it was less sensitive to suspension depth in the simulation on the particles with gyrotactic as well as gravitactic features [see tables 3 and 4 in Hopkins and Fauci (Hopkins and Fauci, 2002)]. Simulations also showed that the wave number was smaller in 'purely geotactic' cells. The results of these simulations suggest that the gyrotactic feature is a potential factor explaining the different characteristics found between the pattern of onset and that of SS1 and SS2.

At onset, overturning of the cell accumulation was induced by the instability of the top-heavy stratification. This overturning caused shear flow accompanied by falling plumes, and then initiated the gyrotactic behavior of the cell. The pattern at SS1 may be developed and maintained further by the combination of the gyrotactic and gravitactic features of the cell.

It is therefore likely that the pattern transition response was triggered by the alteration of the balance of gyrotactic and/or gravitactic features. In the two-axis view, the *C. reinhardtii* cells were observed to form steep, concentrated 'beams' and move altogether downwards during the pattern transition response (Fig. 6). This behavior implies the enhancement of the gyrotactic feature of

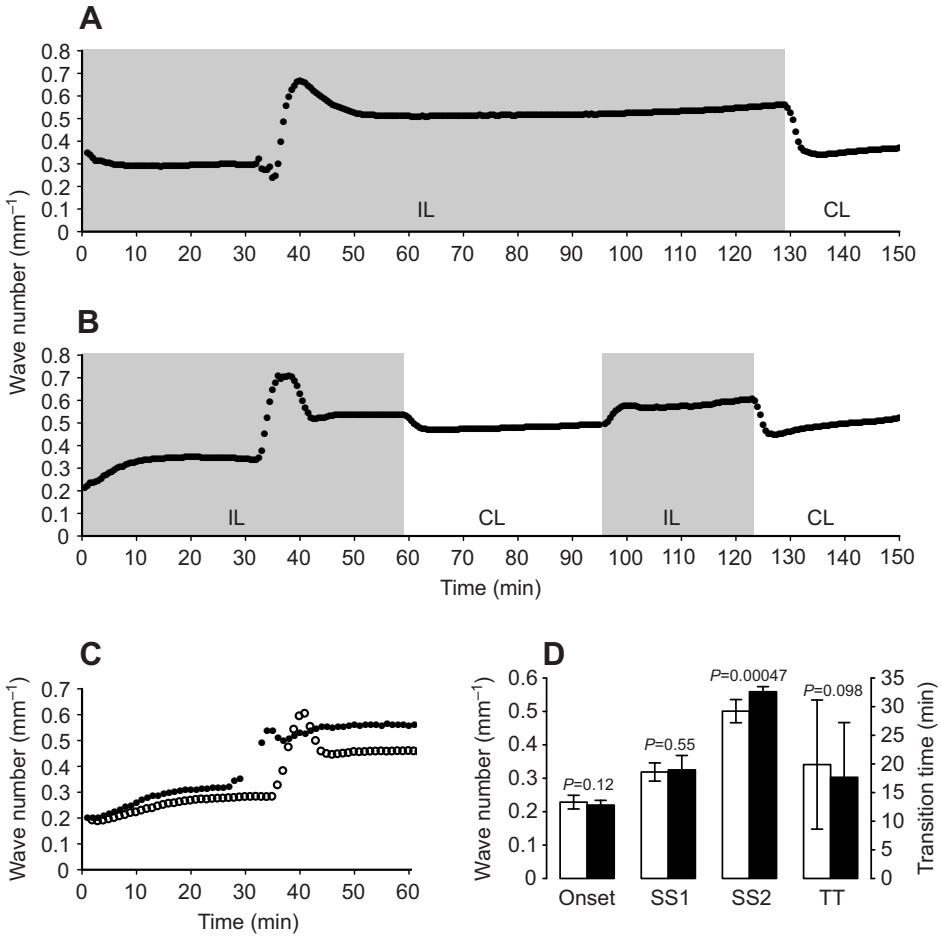

Fig. 7. Light-intensity-dependent changes in the wave number of the bioconvection pattern. (A) Decrease in wave number in response to the change in illumination conditions from intermittent lighting (IL) to continuous lighting (CL). (B) Reversible changes in wave number in response to the change in illumination conditions. (C) Effect of reduced light intensity on the wave number of the pattern before and after the pattern transition response. Two samples from the same batch were illuminated with and without a neutral density (ND) filter and simultaneously recorded. Open circles, specimen illuminated with no ND filter (control); closed circles, specimen illuminated with an ND 0.3 filter (50% of light was cut off). (D) Wave numbers of onset, SS1 and SS2, and the time at which the pattern transition response occurred (TT). White bars, specimen not illuminated with an ND filter (control); black bars, specimen illuminated with an ND 0.3 filter. Data are means ± s.d.

the cell resulting in the entrainment of cells into the downward flow as shown previously (Kessler, 1986a). Hopkins and Fauci reported that gyrotactic cells falling to the bottom in a plume have 'more of a tendency to stay near the bottom of the plume than the purely geotactic cells' (Hopkins and Fauci, 2002). This tendency is in line with our observation that larger populations of cells tended to accumulate at the bottom in SS2 than in SS1 (Fig. 6A, 5 and 15 min). In addition, the visualization of gyrotactic plumes at the 'pseudo-steady-state' [see fig. 9 in Hopkins and Fauci (Hopkins and Fauci, 2002)] appears very similar to our observation of the movement of cell populations during the pattern transition response (Fig. 6A, 12–14 min).

Enhanced gyrotactic features may have forced the larger number of cells to be entrained to the downward plumes, which caused the cell population to shift downward. This may break down the SS1 pattern, and a new pattern may emerge from the disordered, quasi-stable state as the regular pattern, consisting of the 'bottom-standing' plumes with narrower spacing, which is characteristically obtained from the simulated bioconvection of gyrotactic organisms (Ghorai and Hill, 2000). The entrainment of the cell to the downward plume would be accelerated with increasing cell density of the suspension, and result in the shortening of the latent time to the initiation of the pattern transition response (Fig. 5).

Changes in cell shape asymmetry may alter the torque balance

As the gyrotactic instability model states, orientation of the organism toward the flow axis is assumed to be caused by both the gyrotactic and the gravitactic torque (Kessler, 1985b). The gyrotactic torque is generated depending on the vorticity. This torque makes organisms inclined toward the axis of the downward flow. The inclination angle is determined as a balance between the gyrotactic and the gravitactic torques (Kessler, 1985a; Kessler, 1985b; Kessler, 1986b). Enhancement of the gyrotaxis results in an increase in inclination, which is brought about either by an increase of the gyrotactic torque or a decrease of the gravitactic torque.

If the flow velocity field is invariant, the gyrotactic torque increases when the overall geometry of the cell changes to increase the viscous drag coefficient for rotational motion (Kessler, 1986a; Berg, 1993). In contrast, the gravitactic torque decreases, depending on two different mechanisms (Mogami et al., 2001). One is based on the bottom-heavy, fore–aft asymmetry of the internal density, which displaces the center of gravity posterior to the center of buoyancy. Another is based on the bottom-heavy, fore–aft asymmetry of the overall shape, which causes, in low Reynolds number conditions, upward reorientation during sedimentation because the larger posterior part sediments faster than the smaller anterior part of the organism (Roberts, 1970). In the theory of gyrotaxis of *Chlamydomonas*, so far only the density asymmetry has been highlighted because of the fact that immobilized algae continued to orientate upward in the medium of the same density as the algae (Kessler, 1985a). This fact, however, does not exclude the contribution of the shape asymmetry because in the isodense, non-sedimenting conditions, the shape asymmetry fails to generate the torque while the density asymmetry remains functioning. For valid distinction of the mechanisms, specimens should be immersed in the hyperdensity medium, in which shape asymmetry causes anterior-down rotation because the larger posterior part floats faster

than the smaller anterior part, while the density asymmetry causes the same anterior-up rotation (Mogami et al., 2001). Hosoya et al. (Hosoya et al., 2010) demonstrated 'positive' gravitaxis and the resultant 'reverse' (inverted) bioconvection of *C. reinhardtii* in hyperdensity medium containing Percoll. This indicates that the fore–aft shape asymmetry is the dominant generator of the gravitactic torque in *C. reinhardtii* rather than the fore–aft density asymmetry. It is therefore highly likely that the changes in shape asymmetry may act either to increase the gyrotactic torque or to decrease the gravitactic torque, both of which would lead to the enhancement of the gyrotaxis of *C. reinhardtii*.

The spherical cell body of *C. reinhardtii* seems hardly deformed because of the presence of the rigid cell wall. Projections of the flagella at the front end of the cell body, in contrast, may contribute greatly to change the fore–aft asymmetry. Roberts (Roberts, 2006) pointed out that flagella have a significant influence on the shape asymmetry for the generation of the gravitactic torque. He also indicated that the effect of the flagella changed dynamically depending on their bending form during a beat cycle. This may support the idea that the fore–aft shape asymmetry could change in close relation to the alteration of the mode of flagellar beating, such as the modification of the coordinated beating of *cis*- and *trans*-flagella (Rüffer and Nultsch, 1987).

Results shown in Fig. 7 indicate that the changes in the tactic features discussed above seem to occur reversibly depending on the intensity of the light of photosynthetically active wavelength. Sineshchekov et al. (Sineshchekov et al., 2000) reported that red light affected the intensity of negative gravitaxis. When irradiated by red light, negative gravitaxis became intense or less marked, depending on the initial levels of tactic behavior. Williams and Bees (Williams and Bees, 2011a), however, reported that the onset pattern wavelength was unresponsive to changes in red light (660 nm), although they used a much greater intensity than that in the present study. It should be stressed that the red-light-induced alteration of the pattern wavelength was found specifically in SS2, and not in onset or in SS1. It is therefore likely that the pattern transition response may occur in association with the physiological changes of the cell responsible for the sensitivity to the illumination intensity, which may be achieved after the transition. Wakabayashi et al. (Wakabayashi et al., 2011) reported that the phototactic response of *C. reinhardtii* was influenced by the redox poise of the cell. It might be possible that changes in the intracellular environment related to photosynthesis trigger the changes in gravitaxis and/or gyrotaxis, which may result in the changes in bioconvection pattern wavelength.

Enhancement of gyrotaxis could be explained in terms of the swimming velocity of the cell. The higher the swimming velocity, the greater the number of cells tends to accumulate in the axis of downward axial flow. This may accelerate the cell suspension to trigger the pattern transition response. In fact, in a previous study (Williams and Bees, 2011b), three linearized models were proposed for photo-gyrotactic bioconvection, which include both gyrotaxis and phototaxis. In one of their models (Model 1), phototaxis is included by modeling cell swimming speed as a function of light intensity. In this model, the mean cell swimming direction is determined separately by balancing gravitational and viscous torques in a stochastic formulation (Williams and Bees, 2011b). Their result indicates that varying the light intensity (and thus the cell swimming speed) did have a significant effect on the pattern wavelength [see fig. 8 in Williams and Bees (Williams and Bees, 2011b)]. Sineshchekov et al. reported that red light affected the velocity of free-swimming *C. reinhardtii* (Sineshchekov et al., 2000). These facts suggest a possible role of swimming velocity in the pattern transition response and the subsequent changes in the pattern wavelength, although we have not yet observed an increase in the swimming velocity of the cell in the bioconvection pattern.

There might be other mechanistic explanations. SS1 and SS2 are both stable convection systems, presumably with SS2 being more stable than SS1. The transition from SS1 to SS2 could be triggered by number density fluctuations in the medium. Another possibility is that cell motility is stimulated during the initial mixing leading to SS1, then switches to SS2 as swimming velocity relaxes.

Conclusions

In the present paper, we present the dynamic behavior of the bioconvection pattern of *C. reinhardtii* that has not been imagined so far. The pattern transition response suggests that the bioconvection pattern has a potential to reorganize its convection structure, even when seemingly stable. This ability for reorganization might allow the bioconvection pattern to respond quickly to environmental cues. Such responsiveness would be assumed from the fact that pattern wavelength changed reversibly depending on the illumination intensity.

It has been pointed out that bioconvection could play some roles in the physiological processes of microorganisms, such as proliferation, germination, nutrient uptake, gas transport and photosynthesis (Noever et al., 1994; Turner, 2000; Ochiai et al., 2011; Williams and Bees, 2011a), although the conclusions of the empirical studies still do not seem to have reached agreement. An experimental study on proliferation claims negative results (Jánosi et al., 2002), while hydrodynamic observation and calculation show that formation of bioconvection should promote oxygen transport (Tuval et al., 2005).

For the assessment of the biological function of bioconvection, dynamic features of the steady-state pattern presented here would be informative. Further studies on the details of the long-term behavior of bioconvection including the pattern transition response are required to clarify the crucial roles of the collective motion in the activity of microorganisms.

AUTHOR CONTRIBUTIONS

A.K. and Y.M. designed the research. A.K. and C.H. conducted the experiments and analyzed the data. A.K. and Y.M. fabricated the experimental equipment. S.A.B. made the tools for the image analysis. A.K., Y.M. and S.A.B. wrote the paper.

COMPETING INTERESTS

The authors declare no competing interests.

FUNDING

This work was supported in part by a grant from the ISAS/JAXA Space Utilization Research Working Group. A.K. is supported by a Research Fellowship for Young Scientists from the Japan Society for the Promotion of Science.

REFERENCES

Akiyama, A., Ookida, A., Mogami, Y. and Baba, S. A. (2005). Spontaneous alteration of the pattern formation in the bioconvection of *Chlamydomonas reinhardtii*. *J. Jpn. Soc. Microgravity Appl.* **22**, 210-215.

Bees, M. A. and Hill, N. A. (1997). Wavelengths of bioconvection patterns. *J. Exp. Biol.* **200**, 1515-1526.

Berg, H. C. (1993). *Random Walks in Biology Expanded Edition*. Princeton, NJ: Princeton University Press.

Childress, W. S., Levandowsky, M. and Spiegel, E. A. (1975). Pattern formation in a suspension of swimming microorganisms: equations and stability theory. *J. Fluid Mech.* **69**, 591-613.

Ghorai, S. and Hill, N. A. (2000). Wavelengths of gyrotactic plumes in bioconvection. *Bull. Math. Biol.* **62**, 429-450.

Harashima, A., Watanabe, M. and Fujishiro, I. (1988). Evolution of bioconvection patterns in a culture of motile flagellates. *Phys. Fluids* **31**, 764-775.

Harris, E. (1989). *The Chlamydomonas Sourcebook*. San Diego, CA: Academic Press.

Hopkins, M. M. and Fauci, L. J. (2002). A computational model of the collective fluid dynamics of motile micro-organisms. *J. Fluid Mech.* **455**, 149-174.

Hosoya, C., Akiyama, A., Kage, A., Baba, S. A. and Mogami, Y. (2010). Reverse bioconvection of *Chlamydomonas* in the hyper-density medium. *Biol. Sci. Space* **24**, 145-152.

Jánosi, I. M., Czirók, A., Silhavy, D. and Holczinger, A. (2002). Is bioconvection enhancing bacterial growth in quiescent environments? *Environ. Microbiol.* **4**, 525-531.

Kage, A., Asato, E., Chiba, Y., Wada, Y., Katsu-Kimura, Y., Kubota, A., Sawai, S., Niihori, M., Baba, S. A. and Mogami, Y. (2011). Gravity-dependent changes in bioconvection of *Tetrahymena* and *Chlamydomonas* during parabolic flight: increases in wave number induced by pre- and post-parabola hypergravity. *Zool. Sci.* **28**, 206-214.

Kessler, J. O. (1985a). Co-operative and concentrative phenomena of swimming micro-organisms. *Contemp. Phys.* **26**, 147-166.

Kessler, J. O. (1985b). Hydrodynamic focusing of motile algal cells. *Nature* **313**, 218-220.

Kessler, J. O. (1986a). The external dynamics of swimming micro-organisms. In *Progress in Phycological Research*, Vol. 4 (ed. F. E. Round), pp. 257-307. Bristol: Biopress.

Kessler, J. O. (1986b). Individual and collective fluid dynamics of swimming cells. *J. Fluid Mech.* **173**, 191-205.

Kitsunezaki, S., Komori, R. and Harumoto, T. (2007). Bioconvection and front formation of *Paramecium tetraurelia*. *Phys. Rev. E Stat. Nonlin. Soft Matter Phys.* **76**, 046301.

Levandowsky, M., Childress, W. S., Spiegel, E. A. and Hutner, S. H. (1975). A mathematical model of pattern formation by swimming microorganisms. *J. Protozool.* **22**, 296-306.

Matsuda, A., Yoshimura, K., Sineshchekov, O. A., Hirono, M. and Kamiya, R. (1998). Isolation and characterization of novel *Chlamydomonas* mutants that display phototaxis but not photophobic response. *Cell Motil. Cytoskeleton* **41**, 353-362.

Mogami, Y., Ishii, J. and Baba, S. A. (2001). Theoretical and experimental dissection of gravity-dependent mechanical orientation in gravitactic microorganisms. *Biol. Bull.* **201**, 26-33.

Mogami, Y., Yamane, A., Gino, A. and Baba, S. A. (2004). Bioconvective pattern formation of *Tetrahymena* under altered gravity. *J. Exp. Biol.* **207**, 3349-3359.

Noever, D. A., Matsos, H. C. and Cronise, R. J. (1994). Bioconvective patterns, topological phase transitions and evidence of self-organized critical states. *Phys. Lett. A* **194**, 295-299.

Ochiai, N., Dragiila, M. I. and Parke, J. L. (2011). Pattern swimming of *Phytophthora citricola* zoospores: an example of microbial bioconvection. *Fungal Biol.* **115**, 228-235.

Roberts, A. M. (1970). Geotaxis in motile micro-organisms. *J. Exp. Biol.* **53**, 687-699.

Roberts, A. M. (2006). Mechanisms of gravitaxis in *Chlamydomonas*. *Biol. Bull.* **210**, 78-80.

Rüffer, U. and Nultsch, W. (1987). Comparison of the beating of cis- and trans-flagella of *Chlamydomonas* cells held on micropipettes. *Cell Motil. Cytoskeleton* **7**, 87-93.

Sineshchekov, O., Lebert, M. and Häder, D. P. (2000). Effects of light on gravitaxis and velocity in *Chlamydomonas reinhardtii*. *J. Plant Physiol.* **157**, 247-254.

Turner, J. S. (2000). *The Extended Organism. The Physiology of Animal-Built Structures.* Cambridge, MA: Harvard University Press.

Tuval, I., Cisneros, L., Dombrowski, C., Wolgemuth, C. W., Kessler, J. O. and Goldstein, R. E. (2005). Bacterial swimming and oxygen transport near contact lines. *Proc. Natl. Acad. Sci. USA* **102**, 2277-2282.

Wager, H. (1911). The effect of gravity upon the movements and aggregation of *Euglena viridis*, Ehrb., and other micro-organisms. *Philos. Trans. R. Soc. B* **201**, 333-390.

Wakabayashi, K., Misawa, Y., Mochiji, S. and Kamiya, R. (2011). Reduction-oxidation poise regulates the sign of phototaxis in *Chlamydomonas reinhardtii*. *Proc. Natl. Acad. Sci. USA* **108**, 11280-11284.

Williams, C. R. and Bees, M. A. (2011a). A tale of three taxes: photo-gyro-gravitactic bioconvection. *J. Exp. Biol.* **214**, 2398-2408.

Williams, C. R. and Bees, M. A. (2011b). Photo-gyrotactic bioconvection. *J. Fluid Mech.* **678**, 41-86.

Yamamoto, Y., Okayama, T., Sato, K. and Takaoki, T. (1992). Relation of pattern formation to external conditions in the flagellate, *Chlamydomonas reinhardtii*. *Eur. J. Protistol.* **28**, 415-420.

Movie 1. Long-term behavior of bioconvection of *Chlamydomonas reinhardtii*, showing the pattern transition response. The same specimen as shown in Fig. 2. Each side of the image is 20 mm. 90 min in real time.

Movie 2. Two-axis view of the pattern transition response in the same specimen as shown in Fig. 6. Upper part, side view (vertical observation); lower part, top view (horizontal observation). 40 min in real time.